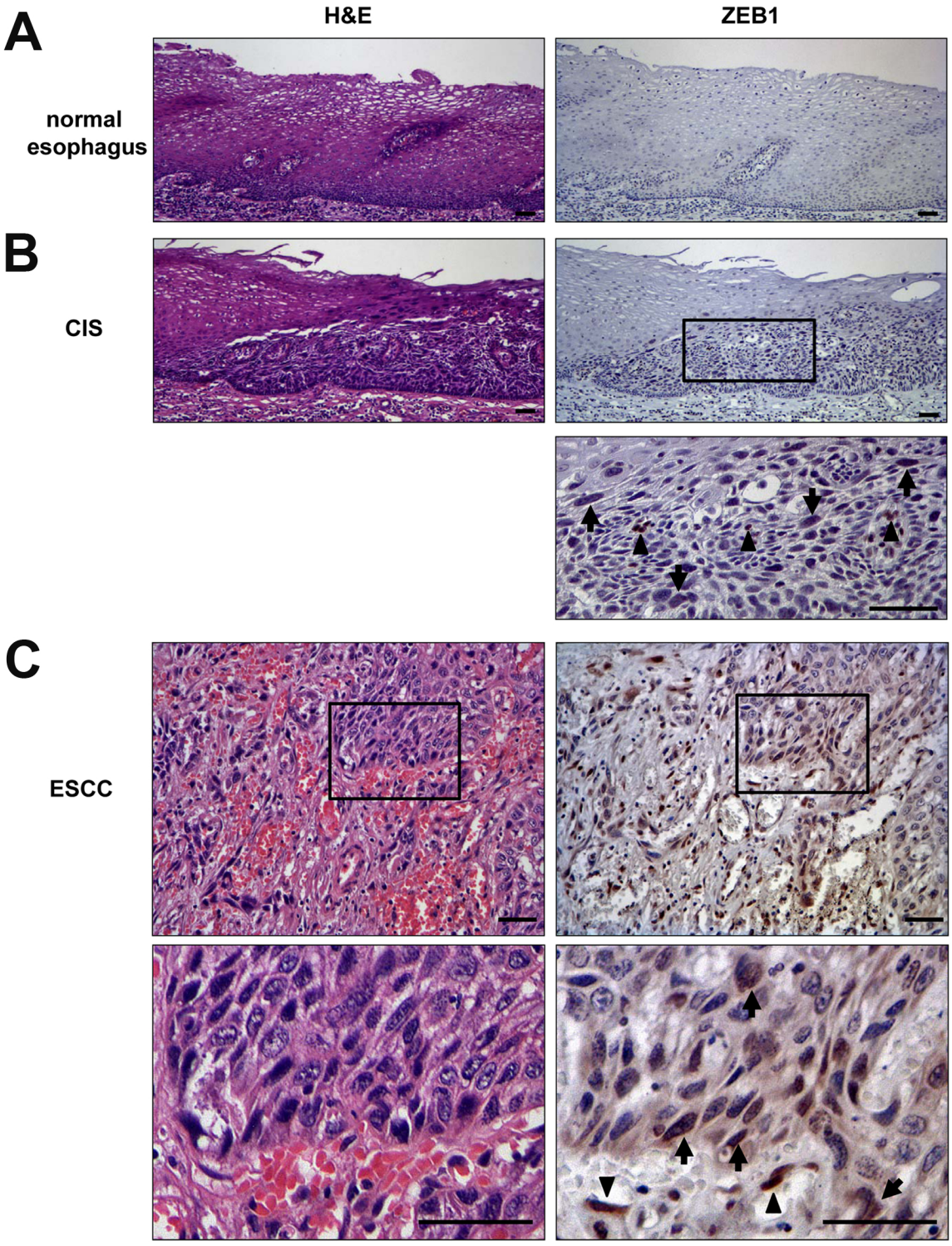

Supplementary Fig. S1 ZEB1 expression in the normal esophageal epithelium, carcinoma *in situ* and invasive ESCC

Representative images for H&E and corresponding IHC in normal mucosa of the esophagus (**A**) carcinoma *in situ* (**B**) and invasive ESCC (**C**). The selected areas were enlarged in the respective lower panels. Note that ZEB1 positive tumor cells tend to be spindle-shaped (arrows). Stromal inflammatory cells and fibroblasts (arrow heads) are also positive for ZEB1. Scale bar, 100 μm.

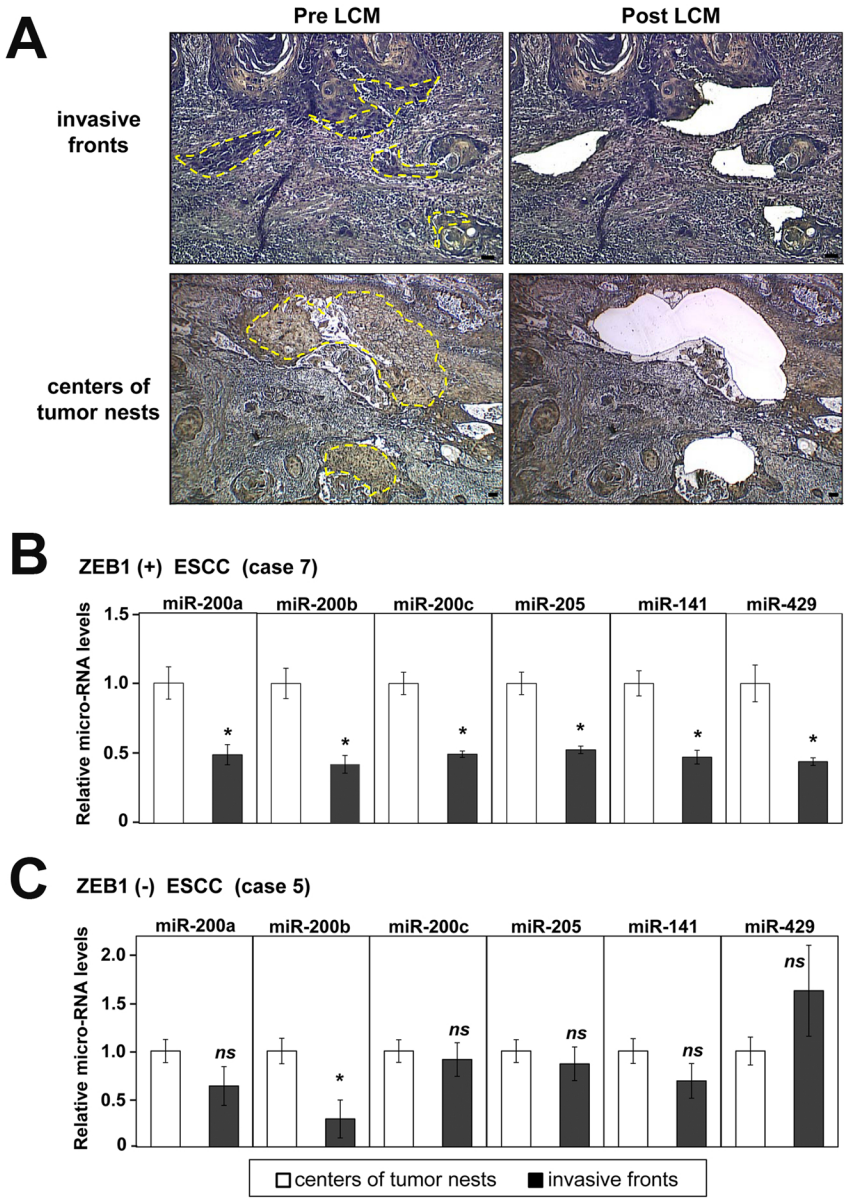

Supplementary Fig. S2 LCM reveals downregulation of the miR-200 family members in the ZEB1-positive invasive fronts of ESCC

A. LCM isolated invasive areas (**top**) and the center of tumor nests (**bottom**) demarcated by yellow broken lines within identical tumors for real-time RT-PCR to compare the expression of the miR-200 family members and related micro-RNAs implicated in negative regulation of ZEBs (i.e. miR-200a, 200b, 200c, 205, 141 and 429).

B. Histograms show miR-200 family expression in a representative ZEB1 positive ESCC sample (case 7 in **Supplementary Table S3**) identical to that used for IHC in **Fig. 1B**. Note that similar results were obtained in two other ZEB1 positive samples tested (not shown). *, $P < 0.01$ versus centers of tumor nests (n=3). Two other ZEB1 positive samples also showed a significant downregulation in at least 5 out of 6 of the miR-200 family and related micro-RNAs tested (data not shown).

C. Histograms show miR-200 family expression in a representative ZEB1 negative ESCC sample (case 5 in **Supplementary Table S3**). Similar results were obtained in two other samples tested (data not shown) where less than 2 out of 6 of the tested microRNAs were significantly downregulated. *, $P < 0.01$ versus centers of tumor nests ns, not significant vs. centers of tumor nests (n=3).

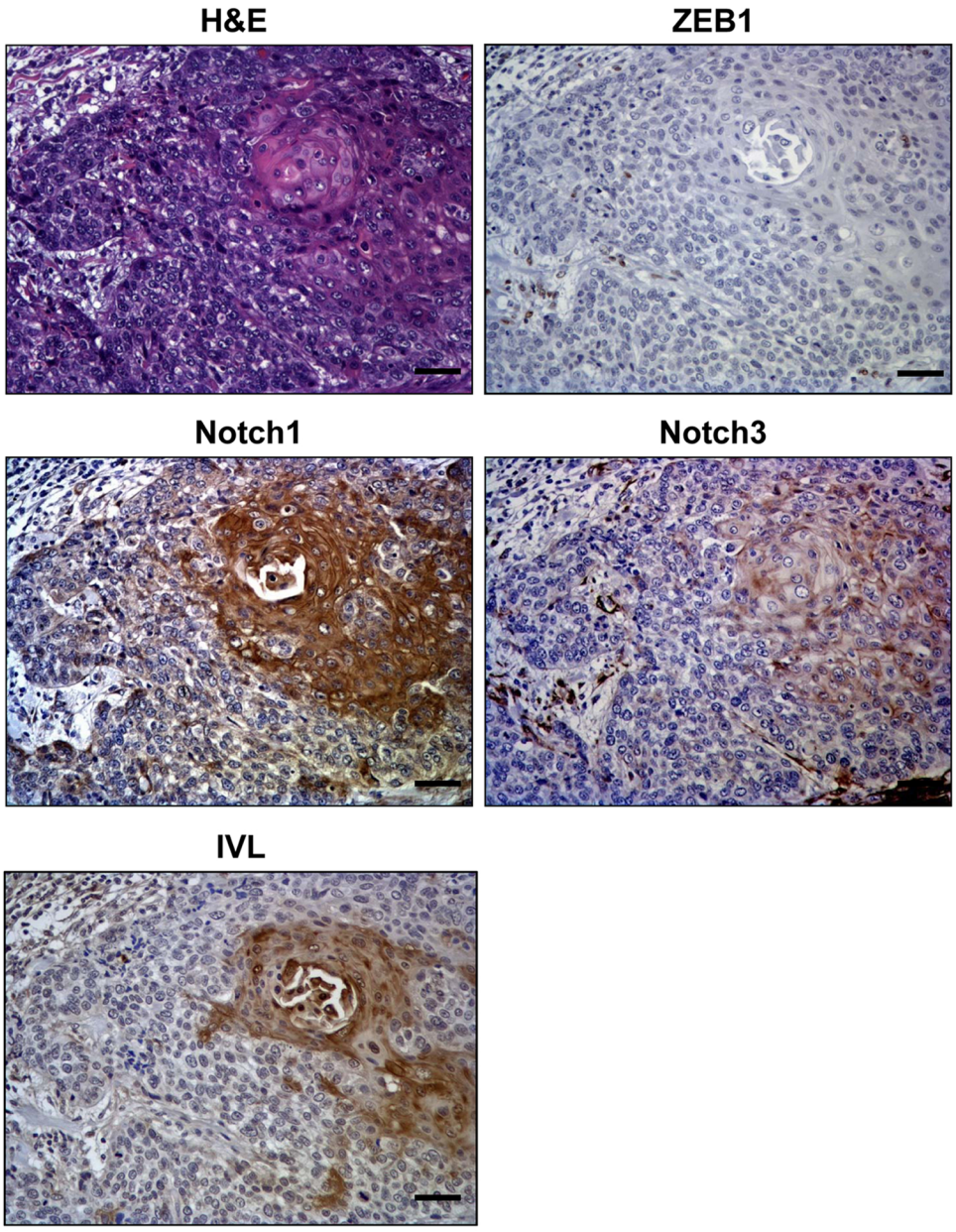

Supplementary Fig. S3 NOTCH1 and NOTCH3 are localized in the well-differentiated tumor nests in ESCC

Representative images for H&E and corresponding IHC on the serial sections. Note that IVL was expressed in the well-differentiated tumor nests forming a keratin pearl surrounded by less-differentiated tumor cells. NOTCH1 and NOTCH3 were co-localized with IVL. ZEB1 was not detected in this sample. Scale bar, 100 μm.

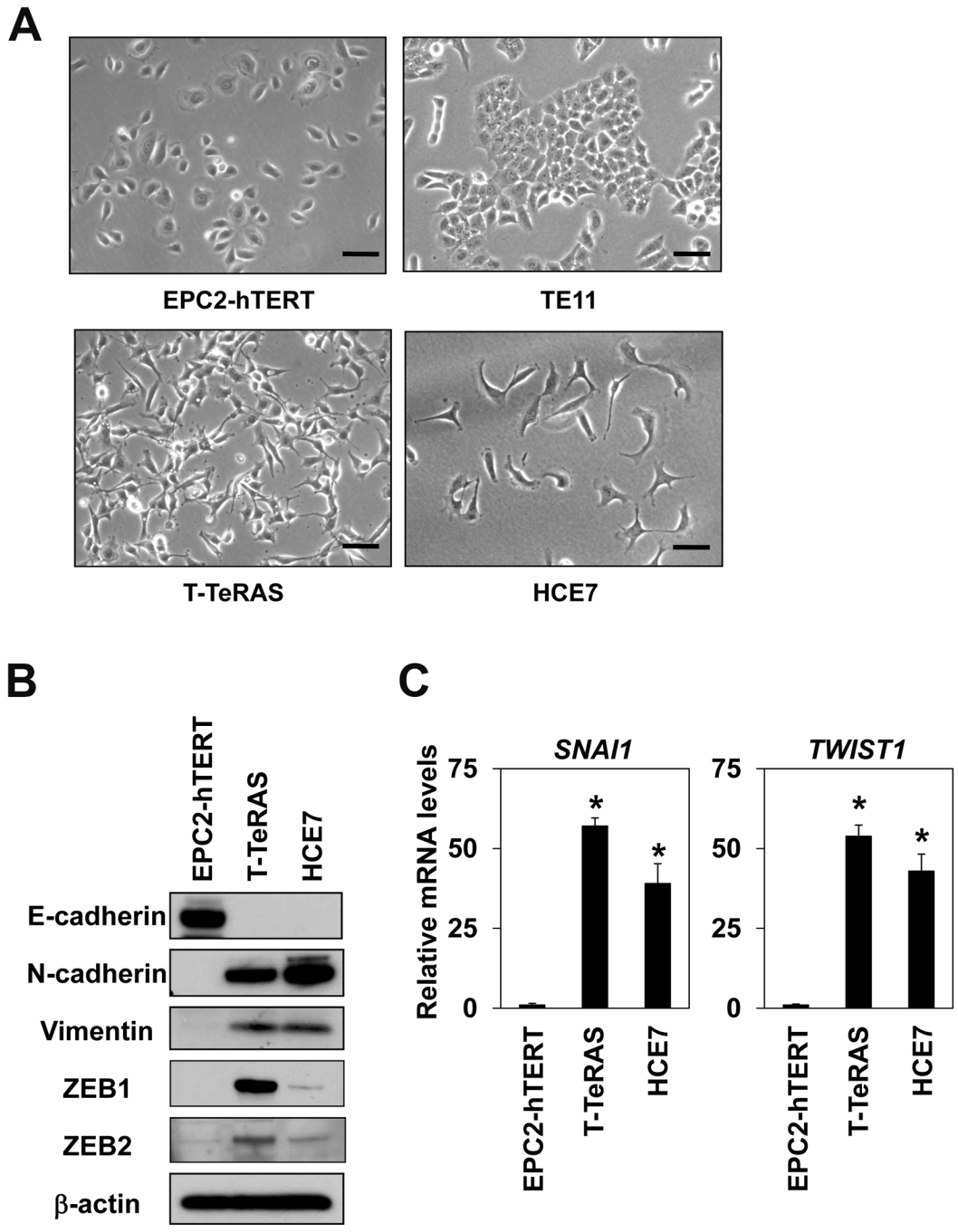

Supplementary Fig. S4 Spindle-shaped morphology and mesenchymal traits in cell lines with upregulation of ZEBs

A. Phase contrast images were taken for indicated cell lines. T-TeRas cells derive from non-transformed EPC2-hTERT cells (6-7). Note that ZEBs were highly expressed in T-TeRAS and HCE7 at the mRNA level (**Fig. 2A**). Unlike TE11 cells with epithelioid-cell appearance, T-TeRAS and HCE7 cells show downregulation of CK13 (**Fig. 2A**), an esophagus-specific early differentiation marker, implying impaired commitment to esophageal squamous differentiation.
Scale bar, 50 μm.
B. Western blotting documents mesenchymal characteristics in T-TeRas and HCE7 cells. β-actin served as a loading control.
C. Quantitative real-time RT-PCR determined relative mRNA levels for indicated genes. β-actin served as an internal control. *, $P< 0.01$ vs. EPC2-hTERT (n=3).

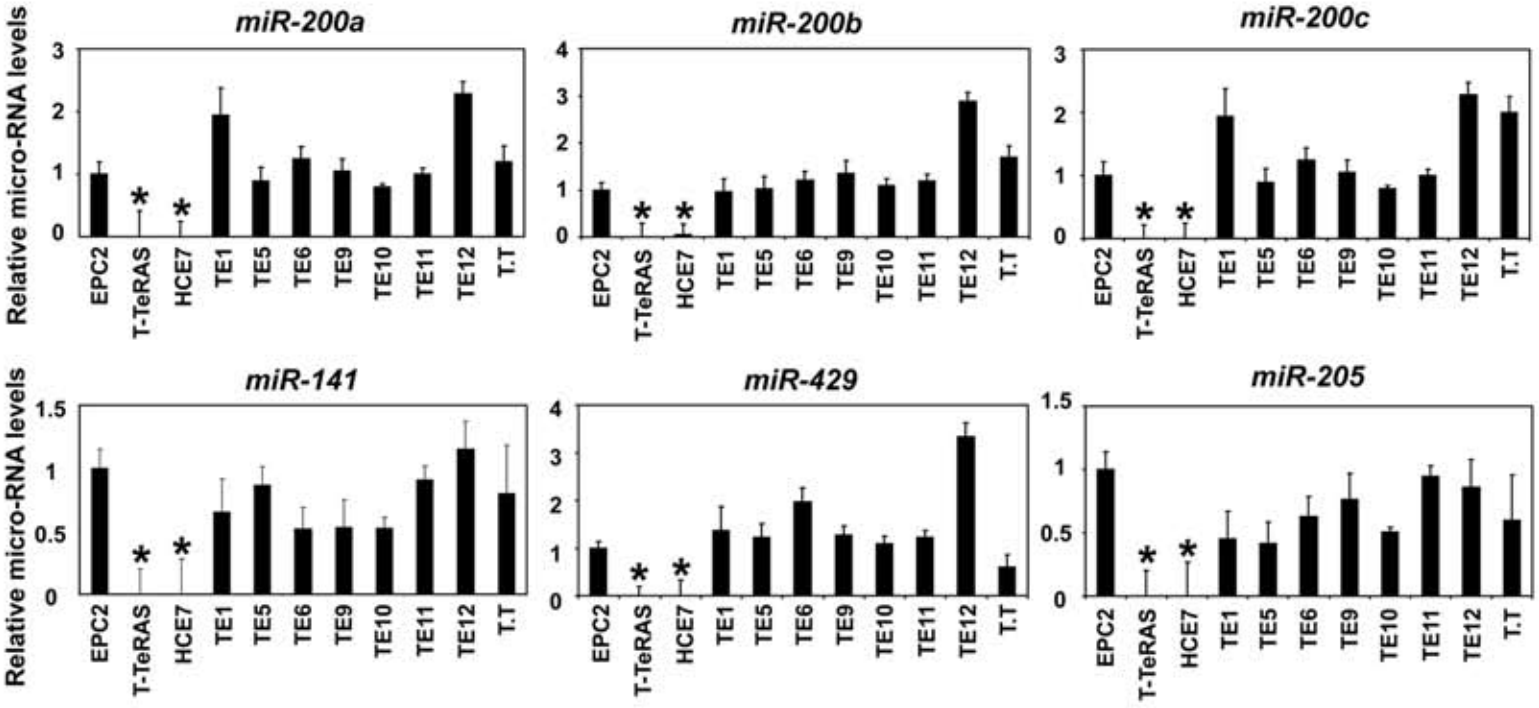

Supplementary Fig. S5 Reciprocal downregulation of the miR-200 family in ESCC cell lines with upregulation of ZEBs

Expression of the miR-200 family members and related micro-RNAs was determined in indicated cell lines by real-time RT-PCR with U47 as an internal control. EPC2, EPC2-hTERT cells. $P < 0.01$ vs. EPC2 (n=3).

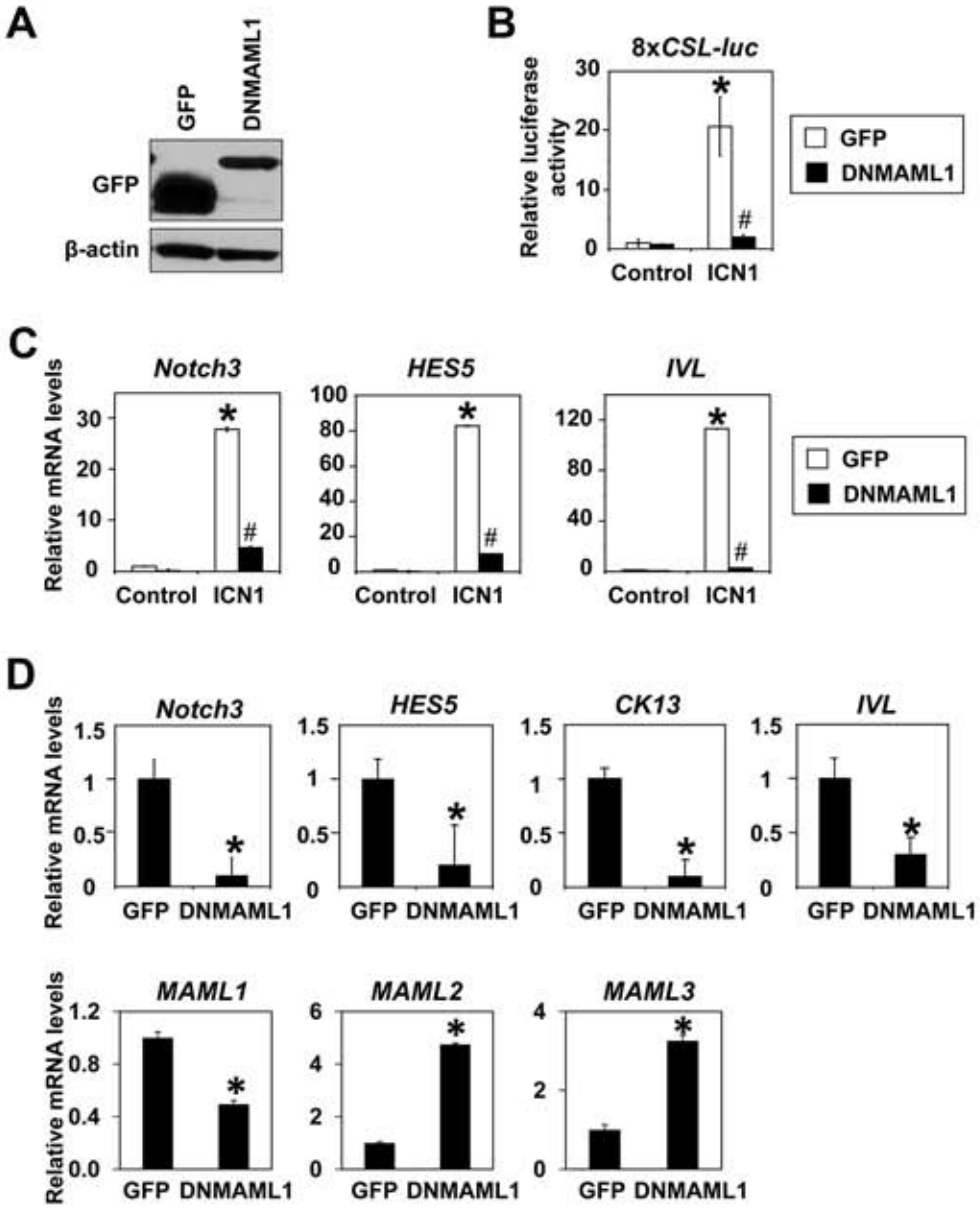

Supplementary Fig. S6 Notch inhibitory effect of DNMAML1 in EPC2-T cells

Functional consequences of DNMAML1 expression upon CSL-dependent transcription as well as induction of Notch target genes were assessed in EPC2-T cells.

A. Western blotting was done on whole cell lysates to document expression of DNMAML1 (GFP-fusion protein) or GFP (control) with an anti-GFP antibody. β-actin served as a loading control.

B. Luciferase assays determined the 8x*CSL-luc* reporter activity by co-transfection of either an ICN1 expression construct (ICN1) or an empty (Control) plasmid in the cells with or without DNMAML1. **P*< 0.001 vs. GFP plus Control; #*P* <0.001 vs. GFP plus ICN1 (n = 6).

C. Real-time RT-PCR determined mRNA for indicated Notch target genes upon ectopic expression of ICN1 by retrovirus-mediated gene transfer. MigR1 (Control) was used as a control. Cells were lysed for RNA purification 3 days after infection.
**P*< 0.001 vs. GFP plus Control; #*P* <0.001 vs. GFP plus ICN1 (n = 3).

D. Real-time RT-PCR determined mRNA for indicated Notch target genes at the basal level in the

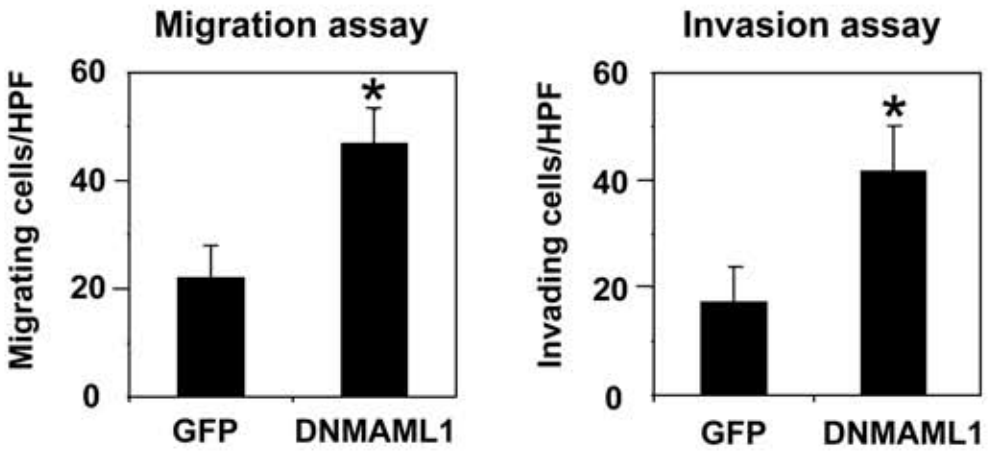

Supplementary Fig. S7 DNMAML1 facilitates cell migration and invasion

Boyden chamber assays determined migration and invasion of EPC2-T ells with or without DNMAML1. *P < 0.01 vs. GFP (n = 3).

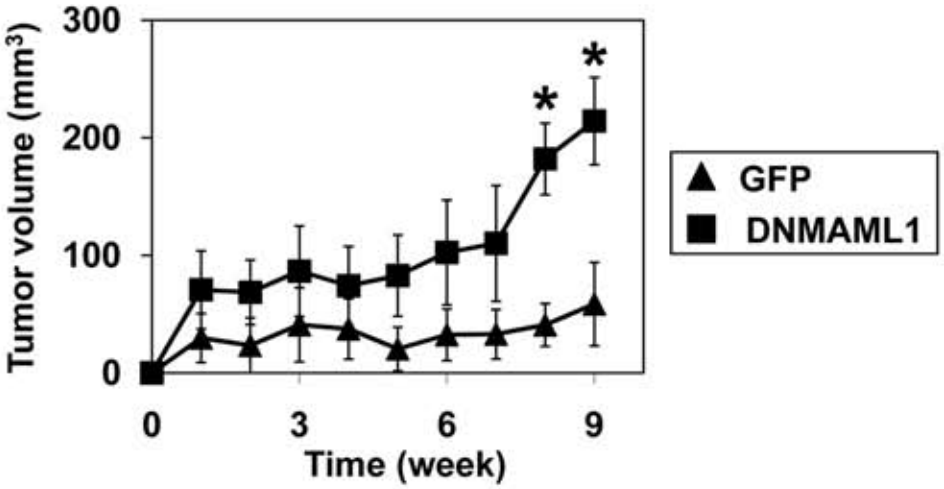

Supplementary Fig. S8 DNMAML1 enhanced xenograft tumor growth

Change in tumor volume was monitored as a function of time in EPC2-T cells with or without DNMAML1. *P < 0.01 vs. GFP (n = 8).

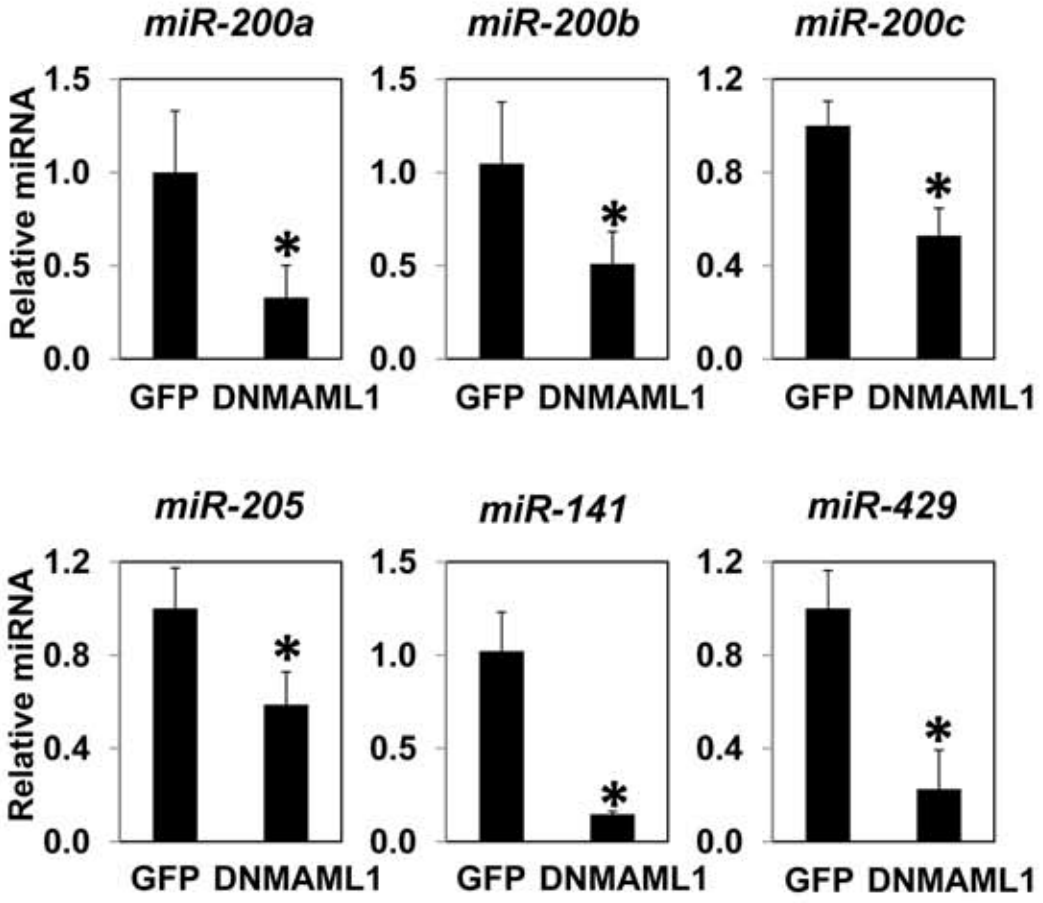

Supplementary Fig. S9 DNMAML1 suppressed the miR-200 family

Expression of the miR-200 family members and related micro-RNAs in EPC2-T cells expressing either DNMAML1 or GFP (control) was determined by real-time RT-PCR with U47 as an internal control. *P*< 0.01 vs. GFP (n=3).

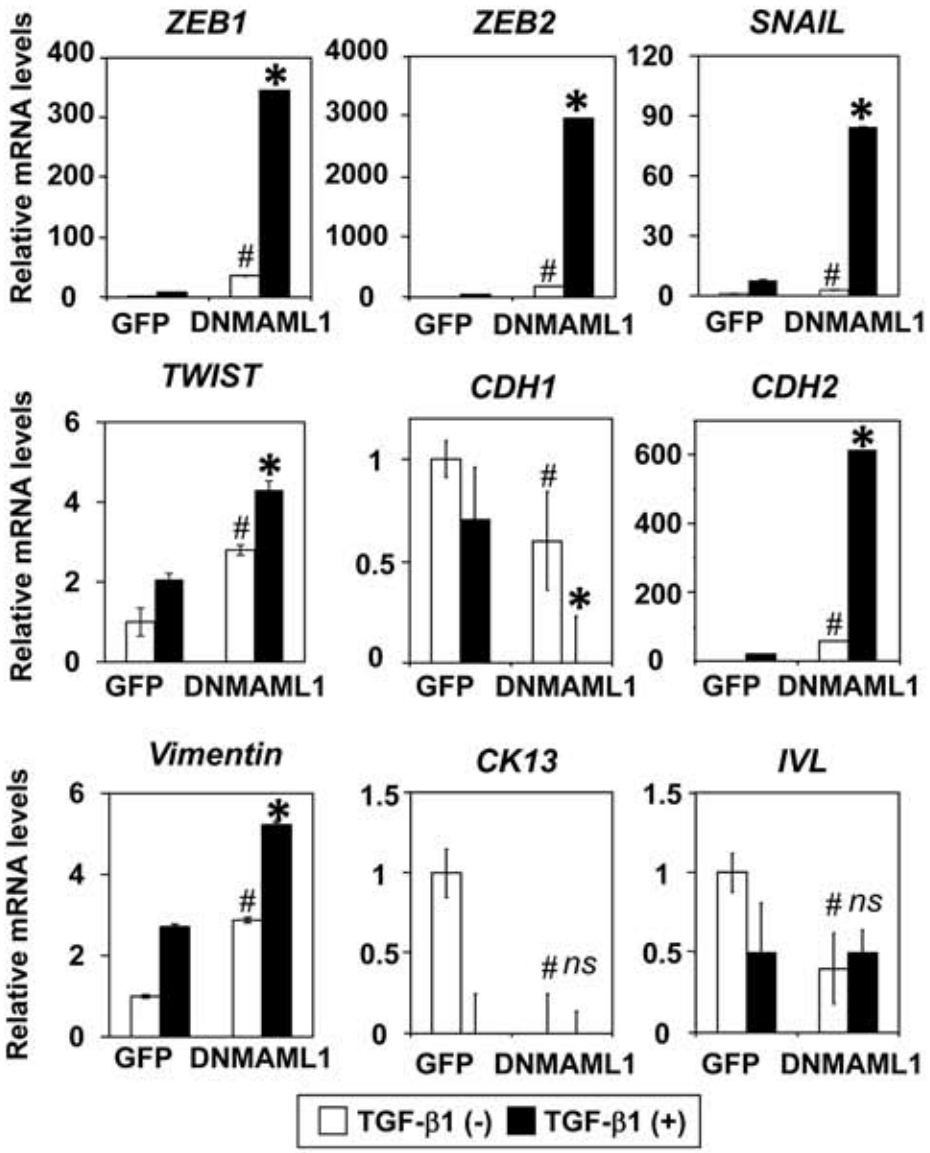

Supplementary Fig. S10 TGF-β1 stimulated ZEBs and EMT markers in the presence of DNMAML1 without promoting squamous cell differentiation.

Real-time RT-PCR determined mRNA for indicated genes in EPC2-T cells expressing either DNMAML1 or GFP (control). β-actin served as an internal control.
CDH1, E-cadherin; *CDH2*, N-cadherin; *, $P < 0.01$ versus GFP plus TGF-β1 (+);
#, $P < 0.05$ versus GFP plus TGF-β1 (-); *ns*, not significant vs. DNMAML1 plus TGF-β1 (-) or GFP plus TGF-β1 (+) (n=3).

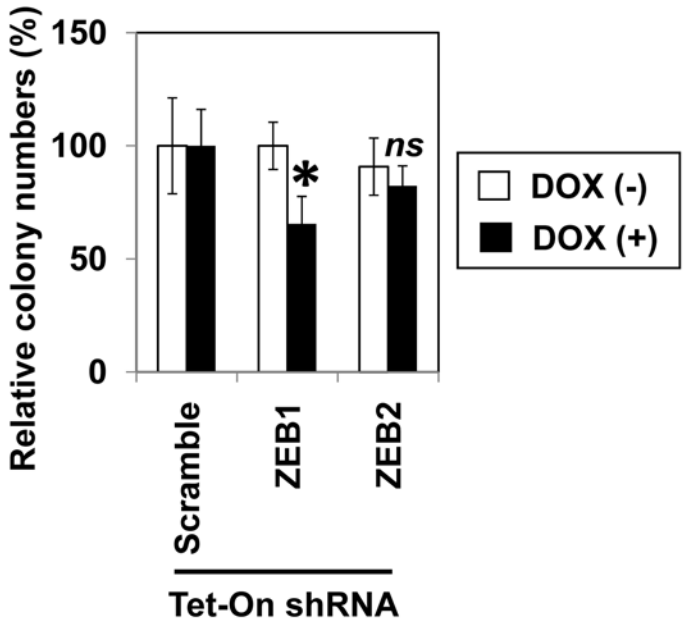

Supplementary Fig. S11 ZEB1 regulates anchorage independent growth of EPC2-T cells with DNMAML1

EPC2-T cells expressing DNMAML1 expressing tetracycline-inducible (Tet-On) shRNA were grown in soft agar in the presence or absence of 1 μg/ml of doxycycline (DOX) for 2 weeks and photomicrographed. Colony number was determined. Representative data are shown with comparable results using two independent shRNA sequences.*, $P < 0.01$ vs. DOX (+) plus scramble; *ns*, vs. DOX (+) plus scramble; n=6. There was no significant change in colony size upon shRNA induction.

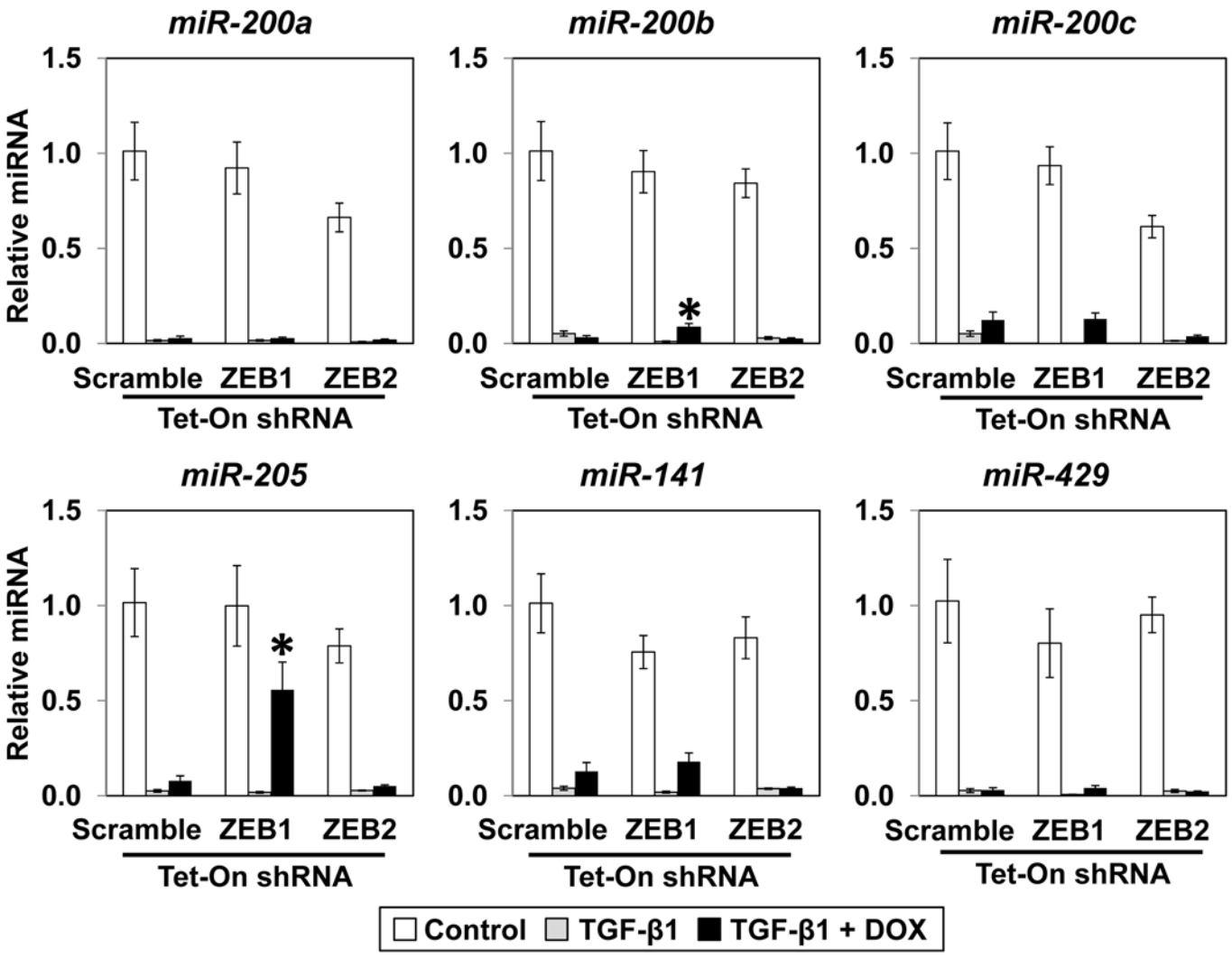

Supplementary Fig. S12 ZEB1 knockdown restores partially the miR-200 family expression in EPC2-T cells with DNMAML1

EPC2-T cells expressing DNMAML1 along with tetracycline-inducible (Tet-On) shRNA directed against either ZEB1, ZEB2 or a non-silence control sequence (Scramble) were subjected to TGF-β1 stimulation along with or without 1 μg/ml of doxycycline (DOX) for 2 weeks as demonstrated in **Fig. 5**. Expression of the miR-200 family members and related micro-RNAs was determined by real-time RT-PCR with U47 as an internal control. Representative data are shown with comparable results using two independent shRNA sequences.
P< 0.01 vs. TGF-β1 plus DOX (+) plus scramble (n=3).

Note that TGF-β1 alone reduced sharply the expression of the miR-200 family. ZEB1 knockdown restored the expression of miR-205 and miR-200b only to a limited extent, implying the involvement of both ZEBs and/or other factors in the miR-200 family regulation.

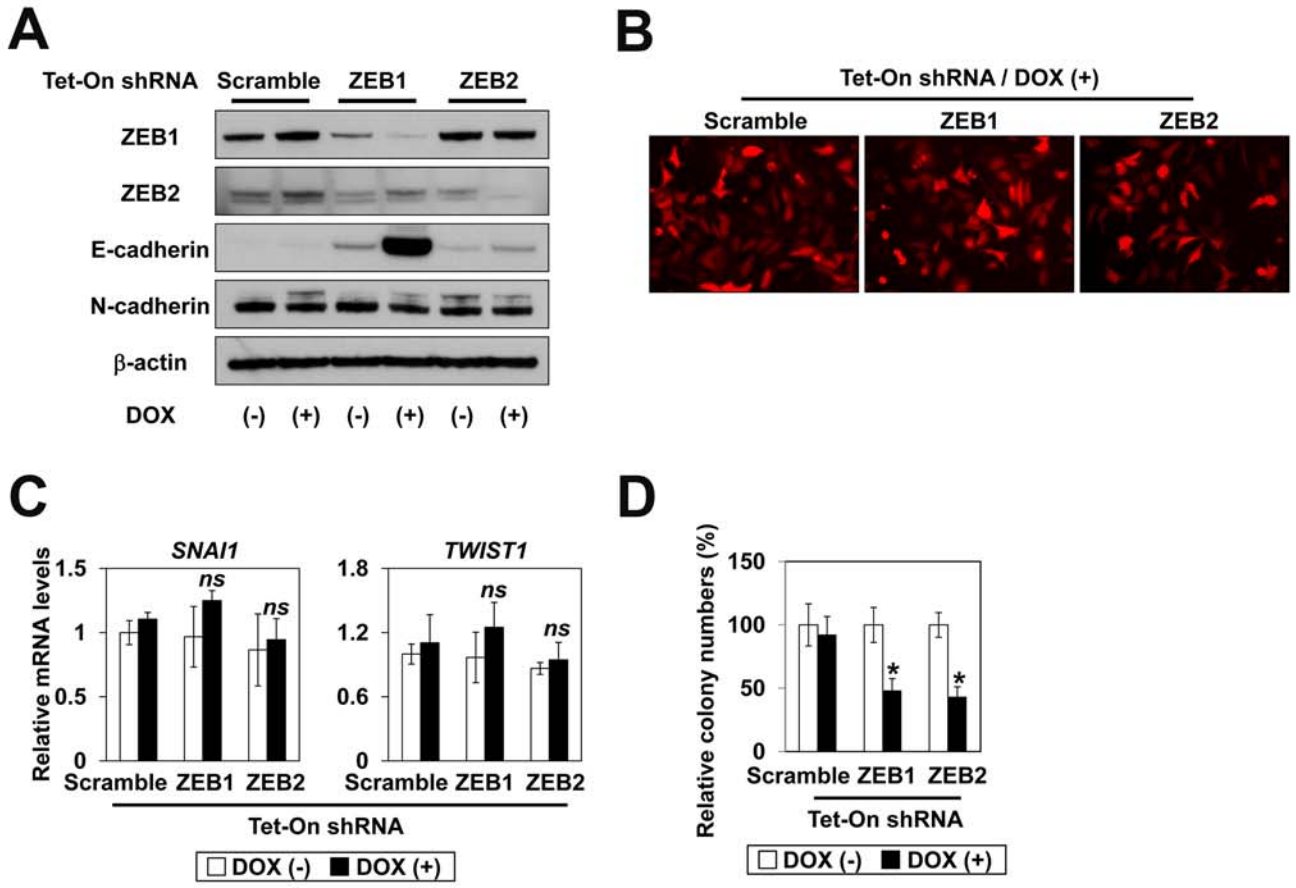

Supplementary Fig. S13 ZEBs represse E-cadherin and regulate anchorage independent growth in HCE7 cells

HCE7 cells expressing tetracycline-inducible (Tet-On) shRNA directed against either ZEB1, ZEB2 or a non-silence control sequence (Scramble) were treated with or without 1 μg/ml of doxycycline (DOX) for 72 hours (**A-C**) and 2 weeks (**D**). HCE7 cells are fully mesenchymal without TGF-β stimulation (**Fig. 2** and **supplementary Fig. S4**). Representative data are shown with comparable results using two independent shRNA sequences.

A. Western blotting determined indicated molecules with β-actin as a loading control. Note that knockdown of ZEB1 induce d E-cadherin robustly compared to knockdown of ZEB2. There was little effect upon N-cadherin expression by knockdown of ZEBs.

B. Fluorescent photomicrographs taken at 72 hrs after DOX treatment documented robust expression of shRNA sequences through co-expressed TurboRFP red fluorescent protein under the tetracycline-operated promoter confirm. No significant morphological change was observed upon knockdown of ZEBs. Flow cytometry also validated TurboRFP induction in > 97% cells (data not shown).

C. Real-time RT-PCR determined mRNA for indicated genes with β-actin as an internal control. ns. not significant vs. scramble plus DOX(+)(n=3). Note that the basal level of *SNAI1* and *TWIST1* in HCE7 cells is high (**supplementary Fig. S4**).

D. Cells were grown in soft agar in the presence or absence of 1 μg/ml of DOX for 2 weeks and photomicrographed to determine colony number. *, $P < 0.01$ vs. DOX (+) plus scramble (n=6). There was no significant change in colony size upon shRNA induction.

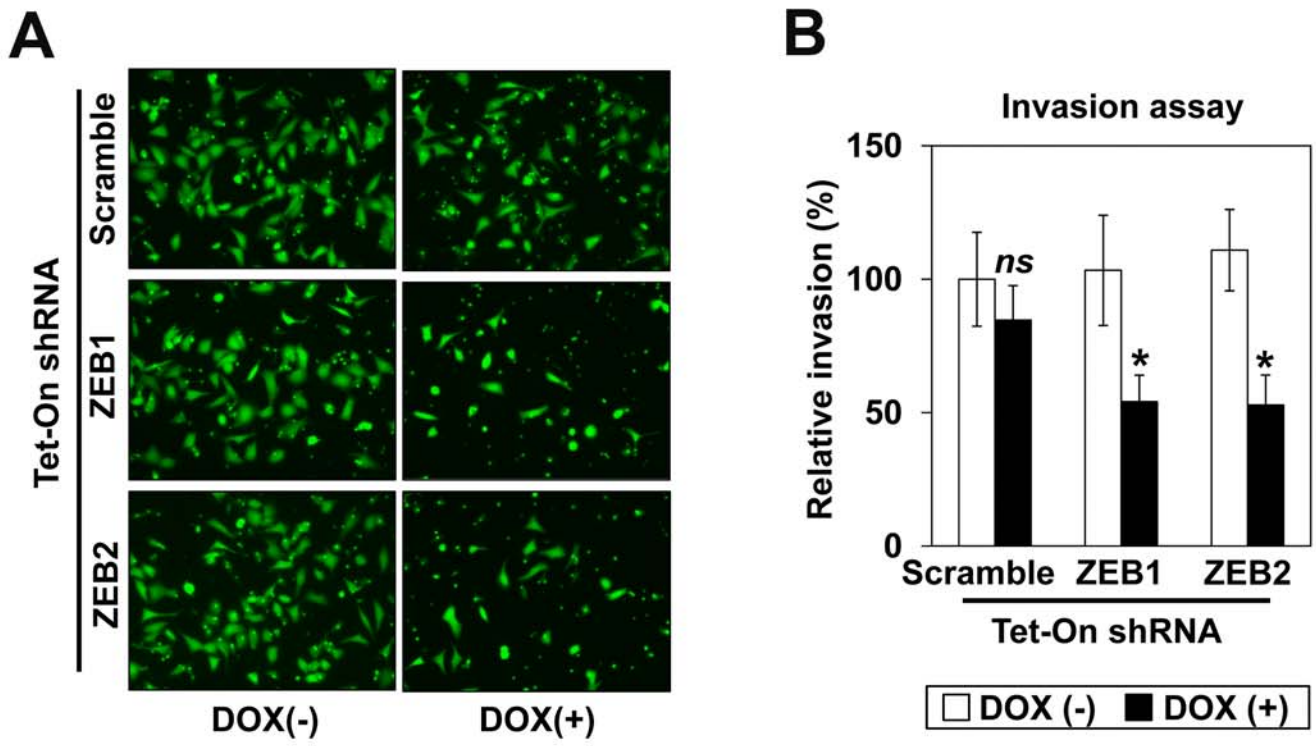

Supplementary Fig. S14 ZEB1 regulates invasion in HCE7 cells

Boyden chamber assays determined invasion of HCE7 cells expressing tetracycline-inducible (Tet-On) shRNA directed against either ZEB1, ZEB2, or a non-silencing control sequence (Scramble). For shRNA induction, cells were pretreated with 1 μg/ml of doxycycline (DOX) for 72 hrs prior to Boyden chamber assays. Cell invasion was monitored in the presence or absence of 1 μg/ml of DOX for 16 hrs. Photomicrograph images of cells stained with Calcein AM dye were shown in (**A**) with an accompanying quantified histogram in (**B**). Representative data are shown with comparable results using two independent shRNA sequences.
*, $P < 0.01$ vs. DOX (+) plus scramble; *ns*, not significant vs. DOX (-); n=3.

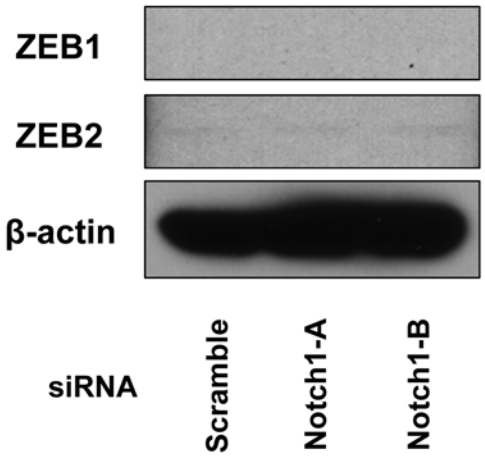

Supplementary Fig. S15 Inhibition of NOTCH1 does not have an immediate impact upon the basal level of ZEB1 and ZEB2.

EPC2-hTERT cells were transiently transfected with siRNA directed against NOTCH1 and subjected to RNA analysis 72 hrs after transfection. Western blotting was done for indicated molecules.
The NOTCH1 knockdown effects upon NOTCH1 per se and NOTCH3 were previously demonstrated at the mRNA and protein levels (1). β-actin served as loading control. Note that ZEB1 and ZEB2 were barely detectable in non-transformed EPC2-hTERT cells .

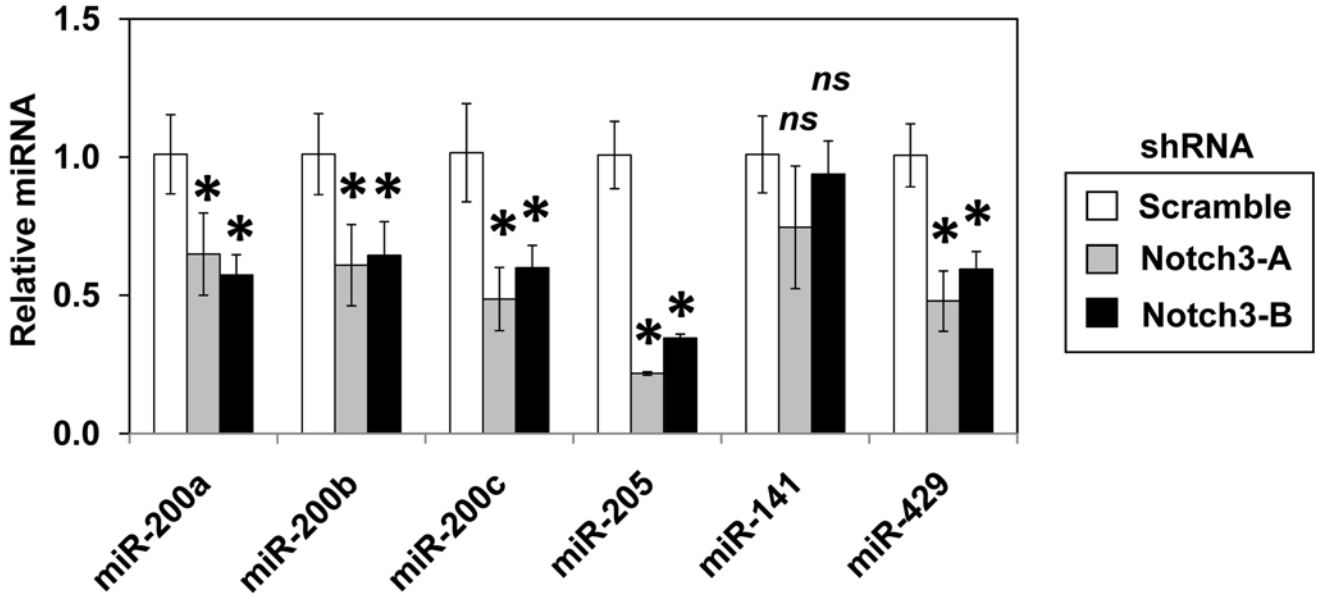

Supplementary Fig. S16 NOTCH3 knockdown suppresses the miR-200 family

Real-time RT-PCR determined the miR-200 family members and related micro-RNAs in EPC2-hTERT derivatives expressing independent shRNA sequences directed against NOTCH3 (Notch3-A and Notch3-B) or a non-silencing control sequence (scramble).
U47 served as an internal control. **, P*< 0.01 vs. scramble; *ns*, not significant vs. scramble (n=3).

Supplementary Methods

Laser capture microdissection (LCM)

LCM was done using the Leica SVS LMD system (Leica Microsystems, Wetzlar, Germany) upon 5μm-thick paraffin embedded ESCC tissue sections. Under the microscopic guidance, Cresyl Violet (Applied Biosystems, Foster City, CA) stained cancer cells at the center of the tumor nests and those at the invasive fronts were selectively dissected, and subjected to Proteinase K treatment 55°C for 12 h and RNA purification with PureLink™ miRNA isolation kit (Invitrogen, Carlsbad, CA, USA).

RNA purified from the LCM samples was subjected to miScript Primer Assays with the miScript SYBR Green PCR Kit for real-time PCR to determine mature miR-200a, miR-200b, miR-200c, miR-205, miR-141 and miR-429 using U6 small nuclear RNA as an inner control according to the manufacturer's instructions.

Luciferase assays

Transient transfection and luciferase assays were done as described previously (1). Briefly, 200 ng of 8x*CSL-luc* (2), a reporter plasmid containing eight copies of the CSL DNA binding consensus sequence was transfected along with either 200 ng of an ICN1 expression vector (3) or a control empty vector (p3XFLAG-CMV-7). Cells were incubated for 48 hrs before cell lysis. The mean of firefly luciferase activity was normalized with the co-transfected renilla luciferase activity.

Migration and invasion assays

Cell migration and invasion assays were done using Boyden chambers as described previously (4-5). In brief, 3 x 10^4 cells were suspended in base medium devoid of growth factors and placed in each insert coated with or without Matrigel matrix (BD Biosciences Co., Franklin, NJ). Cells were allowed to move toward full media filled in the bottom well for 16 hrs and stained with Diff Quick staining kit (Dade Behring, Newark, DE) for EPC2-T cell derivatives and 4 μg/ml Calcein AM dye (Invitrogen) for HCE7 cell derivatives to determine to the moved cells. All Boyden chamber assays were performed at least three times in triplicate.

Supplementary Table S1

Taqman® Gene Expression assays (Applied Biosystems)

IVL, Hs00846307_s1

CK13, Hs00999762_m1

HES5Hs01387463_g1

Notch1, Hs01062014_m1

Notch3, Hs00166432_m1

ZEB1, Hs00232783_m1

ZEB2, Hs00207691_m1

CDH1(E-cadherin), Hs00170423_m1

CDH2(N-cadherin), Hs00983062_m1

Taqman MicroRNA® Assays (Applied Biosystems) used for cultured cells

hsa-miR-200a (000502)

hsa-miR200b (001800)

hsa-miR-200c (000505)

has-miR-141 (000463)

has-miR-205 (000509)

has-miR-429 (001024)

U47 (001223) as an internal control

Supplementary Table S2 Antibodies used

Western blotting

IVL, Mouse monoclonal anti-Involucrin

(CloneSY5)(Sigma-Aldrich, St Louis, MO), Cat# I 9018, (1:1000)

β-actin, Mouse monoclonal anti-β-actin antibody

AC-74 (Sigma Aldrich), Cat# A5316, (1:30,000)

Histone H1, Mouse monoclonal anti-Histone H1 antibody

AE4 (Santa Cruz Biotechnology, Santa Cruz, CA), Cat# sc-8030, (1:250)

GFP, Rabbit polyclonal anti-GFP antibody

(Cell Signaling, Danvers, MA), Cat#2555, (1:1000)

ICN1, Rabbit, monoclonal anti-cleaved NOTCH1 antibody (Val1744)

D3B8 (Cell Signaling), Cat# 4147, (1:1000)

ICN3, Rat monoclonal anti-NOTCH3 antibody

8G5 (Cell Signaling), Cat#3446, (1:1000)

ZEB1, Rabbit monoclonal anti-ZEB1 antibody

D80D3 (Cell Signaling), Cat#3396, (1:1000)

ZEB2, Rabbit polyclonal anti-ZEB2 antibody

H-260 (Santa Cruz), Cat# sc-48789, (1;200)

E-cadherin, Mouse monoclonal anti-E-cadherin antibody

Clone36 (BD Transduction Laboratories, San Jose, CA), Cat#610181, 1:3000

N-cadherin, Mouse monoclonal anti-N-cadherin antibody

Clone 32 (BD Transduction Laboratories), Cat#610920, 1:250

IHC and IF

ZEB1, rabbit serum (8)(1:2000 at 4ºC overnight)/sections microwaved at pH6.0

Notch1, Rabbit polyclonal anti-NOTCH1 antibody (Abcam, Cambridge, MA),

Cat# ab27526, (1:500 at 4ºC overnight)/sections microwaved at pH3.0

Notch3, Rabbit polyclonal anti-NOTCH3 antibody (Abcam)

Cat# ab23426, (1:2000 at 4ºC overnight)/sections microwaved at pH3.0

CK14, Rabbit polyclonal anti-CK14 antibody (Covance),

Cat# PRB-155P, (1:3000 at 4ºC overnight)/sections microwaved at pH6.0

E-cadherin, Mouse monoclonal anti-E-cadherin antibody

Clone36 (BD Transduction Laboratories), Cat#610181, (1:250 at 4ºC overnight)

IVL, Mouse monoclonal anti-involucrin clone Sy5 (Sigma-Aldrich),

Cat# I 9018, (1:750 at 4ºC overnight)/sections microwaved at pH6.0

Note that IHC signals were developed using the diaminobenzidine (DAB) substrate kit (Vector Laboratories, Burlingame, CA) following incubation with secondary anti-mouse IgG (Vector)(1:100 at 37ºC for 30 min) or anti-rabbit IgG (Vector)(1:200 at 37ºC for 30 min), and counterstained with Hematoxylin (Fisher Scientific CS401-1D). For IF, Cyanine Cy2- or Cyanine Cy3-conjugated affinity-purified anti-mouse or anti-rabbit IgG (Jackson ImmunoResearch)(1:600) was used for signal detection by incubating at 37ºC for 30 min, and cell nuclei were counterstained by 4'6-diamidino-2-phenylindole (DAPI)(1:10,000) (Invitrogen).

Supplementary Table S3 Pathological characteristics and ZEB1 staining results of ESCC cases analyzed (n=51)

case#	age/sex	Diff*	pT[a)]	pN[b)]	ZEB1	case#	age/sex	Diff*	pT	pN	ZEB1
1	66M	W	2	0	-	26	55M	M	3	1	-
2	49M	W	3	1	-	27	57M	M	2	1	+
3	66M	P	3	0	-	28	70F	M	1	0	+
4	59M	W	3	2	+	29	75M	W	3	1	+
5	76M	M	3	0	-	30	74M	P	3	1	-
6	76M	M	3	1	-	31	61M	W	3	0	-
7	52M	M	3	1	+	32	53M	M	3	1	-
8	50M	M	2	4	-	33	64M	M	3	1	-
9	64M	M	3	0	-	34	64M	M	4	1	-
10	66M	P	4	U	-	35	54M	M	2	1	-
11	60M	W	1	1	-	36	56M	P	1	1	-
12	80M	M	3	2	-	37	77M	P	3	1	+
13	69M	M	1	2	-	38	71F	W	2	0	-
14	54M	P	3	2	+	39	58M	P	3	1	+
15	62M	M	2	U	-	40	79M	M	3	0	+
16	65M	W	3	0	-	41	57M	M	2	1	+
17	78M	P	3	2	-	42	58M	W	2	1	-
18	76M	M	2	2	-	43	59M	M	3	1	+
19	79M	M	3	2	-	44	68M	P	3	1	+
20	61M	W	3	U	-	45	66M	W	3	1	-
21	62M	M	2	0	-	46	76M	M	3	1	+
22	56M	M	3	1	-	47	60M	M	3	1	-
23	72M	M	2	0	+	48	74M	W	3	1	-
24	57F	M	3	1	+	49	52M	M	3	1	+
25	56M	M	3	1	+	50	63M	M	1	0	-
						51	68F	M	3	1	-

Diff*, differentiation; W, well; M, moderate; P, poor

a) pT; pathologically assessed staging by the size of primary tumor and whether it has invaded nearby tissue

b) pN; pathologically assessed staging by regional lymph nodes that are involved. U, unknown.

Supplementary Table S4 Gene expression profiling in EPC2-hTERT cells expressing shRNA directed against NOTCH3 vs. a non-silencing control sequence

Upregulated (> 10-fold)			Downregulated (> 10-fold)		
Probeset ID	Gene Symbol	Fold-Change	Probeset ID	Gene Symbol	Fold-Change
229152_at	C4orf7	1573.3	213796_at	SPRR1A	-842.2
221731_x_at	VCAN	1081.2	204994_at	MX2	-508.6
212488_at	COL5A1	1006.6	218002_s_at	CXCL14	-498.2
204620_s_at	VCAN	999.3	209230_s_at	NUPR1	-444.9
206336_at	CXCL6	913.0	218990_s_at	SPRR3	-379.4
212489_at	COL5A1	767.0	222484_s_at	CXCL14	-329.0
229273_at	SALL1	667.3	205234_at	SLC16A4	-300.7
208121_s_at	PTPRO	649.8	243754_at	---	-296.0
206026_s_at	TNFAIP6	643.9	227736_at	C10orf99	-277.8
204595_s_at	STC1	598.8	205552_s_at	OAS1	-269.2
213428_s_at	COL6A1	512.4	230835_at	KRTDAP	-215.3
230493_at	SHISA2	490.8	235272_at	SBSN	-202.2
203325_s_at	COL5A1	473.7	1564307_a_at	A2ML1	-195.4
219434_at	TREM1	400.0	229290_at	DAPL1	-190.0
204619_s_at	VCAN	362.1	206714_at	ALOX15B	-156.2
202202_s_at	LAMA4	350.3	202086_at	MX1	-155.3
231532_at	NCAM1	324.1	220403_s_at	TP53AIP1	-132.6
204421_s_at	FGF2	305.4	239430_at	IGFL1	-131.6
244552_at	ZNF788	284.8	231928_at	HES2	-128.4
227394_at	NCAM1	282.0	204439_at	IFI44L	-126.2
226705_at	FGFR1	251.6	239370_at	---	-120.1
205207_at	IL6	250.2	219909_at	MMP28	-118.7
226769_at	FIBIN	242.9	204533_at	CXCL10	-110.2
212915_at	PDZRN3	242.3	215125_s_at	UGT1A1[#1]	-108.6
224964_s_at	GNG2	242.2	205863_at	S100A12	-106.2
212843_at	NCAM1	239.7	218559_s_at	MAFB	-105.0
1554199_at	PTPRO	235.6	211597_s_at	HOPX	-103.4
212681_at	EPB41L3	209.7	236119_s_at	SPRR2G	-103.1
206025_s_at	TNFAIP6	199.6	206094_x_at	UGT1A1[#1]	-96.9
242651_at	---	192.4	204532_x_at	UGT1A1[#2]	-96.5
214043_at	PTPRD	175.6	206008_at	TGM1	-95.3
226322_at	TMTC1	160.7	209596_at	MXRA5	-94.7
215646_s_at	VCAN	156.7	207126_x_at	UGT1A1[#2]	-93.6
211571_s_at	VCAN	148.2	239381_at	KLK7	-93.2
229485_x_at	SHISA3	144.7	223919_at	TP53AIP1	-89.6

Upregulated (> 10-fold)			Downregulated (> 10-fold)		
206290_s_at	RGS7	139.2	232082_x_at	SPRR3	-85.7
228186_s_at	RSPO3	134.6	219684_at	RTP4	-83.2
221107_at	CHRNA9	133.0	211122_s_at	CXCL11	-81.7
1554997_a_at	PTGS2	129.9	206101_at	ECM2	-81.4
208394_x_at	ESM1	123.4	1554179_s_at	LYNX1	-77.4
225202_at	RHOBTB3	118.6	1569787_at	RFTN1	-71.2
207442_at	CSF3	118.6	232277_at	---	-70.6
218469_at	GREM1	113.3	209792_s_at	KLK10	-67.9
226610_at	CENPV	108.8	202869_at	OAS1	-66.0
202976_s_at	RHOBTB3	100.6	218182_s_at	CLDN1	-65.3
206508_at	CD70	98.9	223832_s_at	CAPNS2	-62.8
239468_at	MKX	89.0	242204_at	WFDC5	-62.4
203708_at	PDE4B	88.5	212977_at	CXCR7	-60.5
235759_at	---	87.5	206125_s_at	KLK8	-60.0
213817_at	IRAK3	86.5	229327_s_at	---	-58.4
201721_s_at	LAPTM5	81.9	206517_at	CDH16	-57.0
204597_x_at	STC1	78.4	222549_at	CLDN1	-56.7
226931_at	TMTC1	75.9	208596_s_at	UGT1A1[#1]	-54.9
228116_at	DUXAP10	71.3	226702_at	CMPK2	-54.9
205100_at	GFPT2	71.2	223634_at	RASD2	-54.8
226611_s_at	CENPV	70.9	223920_s_at	TP53AIP1	-54.3
230746_s_at	LOC100288985	69.7	236534_at	BNIPL	-54.1
212764_at	ZEB1	68.8	205470_s_at	KLK11	-53.9
205825_at	PCSK1	68.7	210163_at	CXCL11	-53.3
219295_s_at	PCOLCE2	67.9	242625_at	RSAD2	-53.1
219132_at	PELI2	66.7	219593_at	SLC15A3	-52.1
228107_at	LOC100127983	66.0	243271_at	---	-51.8
242546_at	FLJ39632	63.4	1558764_at	---	-51.5
206204_at	GRB14	62.3	219962_at	ACE2	-50.1
218468_s_at	GREM1	61.2	222257_s_at	ACE2	-49.9
218976_at	DNAJC12	61.0	205185_at	SPINK5	-49.8
221911_at	ETV1	60.5	204747_at	IFIT3	-48.0
201262_s_at	BGN	60.4	213332_at	PAPPA2	-46.1
206710_s_at	EPB41L3	60.4	241417_at	---	-46.0
211506_s_at	IL8	59.8	218999_at	TMEM140	-45.5
228333_at	ZEB2	59.5	226560_at	---	-44.9
205381_at	LRRC17	58.7	208539_x_at	SPRR2B	-43.9
203131_at	PDGFRA	58.6	203281_s_at	UBA7	-43.5
210139_s_at	PMP22	57.6	206363_at	MAF	-43.4

Upregulated (> 10-fold)			Downregulated (> 10-fold)		
207569_at	ROS1	57.2	1569453_a_at	LOC692247	-43.4
204422_s_at	FGF2	54.5	209794_at	SRGAP3	-43.1
1557961_s_at	LOC100127983	52.9	223502_s_at	TNFSF13B	-43.0
223721_s_at	DNAJC12	52.6	204942_s_at	ALDH3B2	-42.9
209199_s_at	MEF2C	51.7	39249_at	AQP3	-42.9
212813_at	JAM3	51.1	202357_s_at	CFB	-41.4
229288_at	EPHA7	50.7	209800_at	KRT16	-41.0
209200_at	MEF2C	50.2	1553906_s_at	FGD2	-41.0
235343_at	VASH2	49.4	240284_x_at	EMG1	-40.9
207558_s_at	PITX2	49.1	214059_at	IFI44	-40.6
242860_at	---	48.4	204415_at	IFI6	-40.1
336_at	TBXA2R	47.0	227128_s_at	---	-40.1
1556138_a_at	COL5A1	45.8	217497_at	TYMP	-39.7
1560490_at	FAT3	45.6	227735_s_at	C10orf99	-39.6
204596_s_at	STC1	45.3	219554_at	RHCG	-39.5
208937_s_at	ID1	43.4	213797_at	RSAD2	-38.8
206018_at	FOXG1	43.2	229385_s_at	PLAC2	-38.4
244363_at	ROS1	42.9	201641_at	BST2	-36.8
219249_s_at	FKBP10	42.7	227717_at	ARHGEF37	-36.8
222686_s_at	CPPED1	42.1	232056_at	SCEL	-36.2
224397_s_at	TMTC1	41.9	230233_at	---	-36.2
226625_at	TGFBR3	41.4	207571_x_at	C1orf38	-36.1
230147_at	F2RL2	40.8	228486_at	SLC44A1	-35.7
218541_s_at	C8orf4	40.7	213348_at	CDKN1C	-35.6
201578_at	PODXL	39.7	225803_at	FBXO32	-35.5
205081_at	CRIP1	39.2	211002_s_at	TRIM29	-35.0
206835_at	STATH	39.1	220120_s_at	EPB41L4A	-34.4
223614_at	MMP16	39.1	214599_at	IVL	-33.8
1557326_at	LOC100130911	38.8	227609_at	EPSTI1	-33.8
215112_x_at	MCF2L2	38.4	1552319_a_at	KLK8	-33.7
203440_at	CDH2	38.3	223075_s_at	AIF1L	-33.3
235696_at	---	38.2	211361_s_at	SERPINB13	-33.3
242069_at	CBX5	38.1	220402_at	TP53AIP1	-33.1
206893_at	SALL1	38.1	224482_s_at	RAB11FIP4	-32.8
229088_at	ENPP1	37.5	231033_at	---	-32.8
203685_at	BCL2	36.5	217502_at	IFIT2	-32.4
233030_at	PNPLA3	36.3	206561_s_at	AKR1B10	-32.3
228653_at	SAMD5	36.0	232375_at	---	-32.1
211776_s_at	EPB41L3	36.0	239582_at	PML	-32.1
218610_s_at	CPPED1	35.5	229555_at	GALNT5	-32.0

Upregulated (> 10-fold)			Downregulated (> 10-fold)		
1559725_at	---	35.3	206553_at	OAS2	-31.9
230351_at	LOC283481	34.1	210785_s_at	C1orf38	-31.8
223253_at	EPDR1	34.0	205749_at	CYP1A1	-31.6
213610_s_at	KLHL23	33.4	1558765_a_at	---	-31.5
219740_at	VASH2	33.0	206400_at	LGALS7[#3]	-31.3
244463_at	ADAM23	32.9	233565_s_at	SDCBP2	-31.0
239135_at	CPPED1	32.8	230986_at	KLF8	-30.7
204337_at	RGS4	32.7	209719_x_at	SERPINB3	-30.6
226278_at	SVIP	32.5	219211_at	USP18	-30.5
201261_x_at	BGN	32.4	203407_at	PPL	-30.2
231040_at	---	31.4	203153_at	IFIT1	-29.9
228128_x_at	PAPPA	31.2	224328_s_at	LCE3D	-29.9
206985_at	HSD17B3	30.6	210086_at	HR	-29.5
231001_at	FIBIN	30.5	232165_at	EPPK1	-28.9
206837_at	ALX1	30.4	207366_at	KCNS1	-28.8
236029_at	FAT3	30.4	228010_at	PPP2R2C	-28.7
242346_x_at	---	30.3	215465_at	ABCA12	-28.6
203603_s_at	ZEB2	30.0	225328_at	---	-28.5
206953_s_at	LPHN2	29.8	AFFX-HUMISGF3A/M97935_MA_at	STAT1	-28.4
242939_at	TFDP1	29.5	206082_at	HCP5	-27.7
225784_s_at	ZC4H2	29.2	1556643_at	FAM125A	-27.7
1569583_at	EREG	29.0	204638_at	ACP5	-27.4
228956_at	UGT8	28.9	222838_at	SLAMF7	-27.4
214954_at	SUSD5	28.9	230076_at	PITPNM3	-27.2
230436_s_at	CENPV	28.6	226474_at	NLRC5	-27.1
226210_s_at	MEG3	27.6	210797_s_at	OASL	-27.0
206157_at	PTX3	27.1	206884_s_at	SCEL	-27.0
201893_x_at	DCN	26.8	206191_at	ENTPD3	-26.9
220040_x_at	ZC4H2	26.6	235276_at	EPSTI1	-26.9
224965_at	GNG2	26.3	236359_at	SCN4B	-26.8
219985_at	HS3ST3A1	26.2	222242_s_at	KLK5	-26.5
206504_at	CYP24A1	26.1	220432_s_at	CYP39A1	-26.3
208893_s_at	DUSP6	26.0	238327_at	ODF3B	-26.3
223722_at	DNAJC12	25.8	209030_s_at	CADM1	-26.3
232636_at	SLITRK4	24.8	1553505_at	A2ML1	-26.2
206172_at	IL13RA2	24.3	201249_at	SLC2A1	-26.1
225275_at	EDIL3	24.3	1294_at	UBA7	-25.6
205826_at	MYOM2	24.1	232164_s_at	EPPK1	-25.5
1554036_at	ZBTB24	23.9	230314_at	---	-25.1

Upregulated (> 10-fold)			Downregulated (> 10-fold)		
204749_at	NAP1L3	23.7	202488_s_at	FXYD3	-25.0
208307_at	RBMY1A1[#4]	23.7	226932_at	SSPN	-24.7
242881_x_at	---	23.3	223720_at	SPINK7	-24.7
207437_at	NOVA1	23.2	221013_s_at	APOL2	-24.6
205794_s_at	NOVA1	23.2	43427_at	ACACB	-24.4
204880_at	MGMT	23.1	214797_s_at	CDK18	-24.0
228737_at	TOX2	22.7	220322_at	IL1F9	-23.6
207761_s_at	METTL7A	22.5	203747_at	AQP3	-23.4
232027_at	SYNE1	21.9	217272_s_at	SERPINB13	-22.8
242486_at	---	21.5	208161_s_at	ABCC3	-22.7
224507_s_at	MGC12916	21.5	225728_at	SORBS2	-22.7
201981_at	PAPPA	21.4	221698_s_at	CLEC7A	-22.4
210089_s_at	LAMA4	21.2	1559607_s_at	GBP6	-22.3
213905_x_at	BGN	20.6	230266_at	RAB7B	-22.0
202435_s_at	CYP1B1	20.6	214475_x_at	CAPN3	-21.9
218974_at	SOBP	20.5	227266_s_at	FYB	-21.8
224940_s_at	PAPPA	20.4	226403_at	TMC4	-21.8
228218_at	LSAMP	20.4	214549_x_at	SPRR1A	-21.7
203980_at	FABP4	20.2	232116_at	GRHL3	-21.6
230003_at	---	20.1	210895_s_at	CD86	-21.6
209406_at	BAG2	20.1	203238_s_at	NOTCH3	-21.5
239033_at	---	20.0	235643_at	SAMD9L	-21.5
205830_at	CLGN	19.6	236172_at	LTB4R	-21.3
202975_s_at	RHOBTB3	19.6	219091_s_at	MMRN2	-21.3
202436_s_at	CYP1B1	19.5	1555759_a_at	CCL5	-21.3
204947_at	E2F1	19.4	235175_at	GBP4	-21.1
225627_s_at	CACHD1	19.4	202575_at	CRABP2	-21.1
228461_at	SH3RF3	19.3	209032_s_at	CADM1	-21.1
213362_at	PTPRD	19.0	202790_at	CLDN7	-21.0
232504_at	LOC285628	18.9	242354_at	---	-20.9
230744_at	FSTL1	18.8	230708_at	PRICKLE1	-20.9
229975_at	BMPR1B	18.5	208436_s_at	IRF7	-20.8
1567223_at	HMGA2	18.4	229396_at	OVOL1	-20.7
204011_at	SPRY2	18.4	206133_at	XAF1	-20.7
239942_at	---	18.1	231068_at	SLC47A2	-20.5
242579_at	BMPR1B	18.0	207708_at	ALOXE3	-20.5
243597_at	FANCB	18.0	230075_at	RAB39B	-20.5
213316_at	KIAA1462	17.9	209919_x_at	GGT1	-20.3
207057_at	SLC16A7	17.9	221680_s_at	ETV7	-20.3
241925_x_at	---	17.8	226213_at	ERBB3	-20.2

Upregulated (> 10-fold)			Downregulated (> 10-fold)		
2028_s_at	E2F1	17.7	1568932_at	---	-20.2
230752_at	---	17.7	228193_s_at	C13orf15	-20.1
209955_s_at	FAP	17.7	203535_at	S100A9	-20.1
202437_s_at	CYP1B1	17.6	238725_at	IRF1	-20.1
230372_at	HAS2	17.4	231148_at	IGFL2	-20.0
215116_s_at	DNM1	17.1	220230_s_at	CYB5R2	-20.0
1554547_at	FAM13C	17.0	211372_s_at	IL1R2	-19.9
203799_at	CD302	16.9	1552584_at	IL12RB1	-19.8
230626_at	TSPAN12	16.9	219209_at	IFIH1	-19.8
203441_s_at	CDH2	16.9	219863_at	HERC5	-19.7
220651_s_at	MCM10	16.7	213261_at	TRANK1	-19.7
230690_at	TUBB1	16.4	221978_at	HLA-F	-19.6
211896_s_at	DCN	16.4	216243_s_at	IL1RN	-19.6
211161_s_at	COL3A1	15.9	220066_at	NOD2	-19.6
212224_at	ALDH1A1	15.8	226069_at	PRICKLE1	-19.3
224941_at	PAPPA	15.6	204963_at	SSPN	-19.1
202947_s_at	GYPC	15.6	222830_at	GRHL1	-19.0
230535_s_at	ATP5E	15.4	207655_s_at	BLNK	-19.0
1562133_x_at	ZNF90	15.4	223501_at	TNFSF13B	-18.9
218921_at	SIGIRR	15.3	205011_at	VWA5A	-18.7
204932_at	TNFRSF11B	15.3	210944_s_at	CAPN3	-18.6
209774_x_at	CXCL2	15.2	1554921_a_at	SCEL	-18.6
238186_at	---	15.1	227642_at	TFCP2L1	-18.6
204235_s_at	GULP1	15.0	236865_at	---	-18.6
202859_x_at	IL8	15.0	228237_at	PAPPA2	-18.5
226751_at	CNRIP1	15.0	228742_at	---	-18.4
212230_at	PPAP2B	14.9	233325_at	SLC35D2	-18.2
209866_s_at	LPHN3	14.9	232105_at	---	-18.2
1555766_a_at	GNG2	14.9	1555416_a_at	ALOX15B	-18.2
204748_at	PTGS2	14.7	205828_at	MMP3	-18.1
230954_at	C20orf112	14.7	220266_s_at	KLF4	-18.1
1554640_at	PALM2	14.6	209969_s_at	STAT1	-18.0
226571_s_at	PTPRS	14.6	207131_x_at	GGT1	-17.9
241866_at	SLC16A7	14.4	228617_at	XAF1	-17.9
206377_at	FOXF2	14.3	219352_at	HERC6	-17.8
219525_at	SLC47A1	14.0	220362_at	PSORS1C1	-17.7
222962_s_at	MCM10	14.0	209031_at	CADM1	-17.7
230585_at	---	14.0	236262_at	MMRN2	-17.6
1567224_at	HMGA2	13.9	239675_at	LOC283143	-17.5
228361_at	E2F2	13.8	241931_at	XG	-17.5

Upregulated (> 10-fold)			Downregulated (> 10-fold)		
204470_at	CXCL1	13.8	230036_at	SAMD9L	-17.5
211813_x_at	DCN	13.8	208392_x_at	SP110	-17.4
216635_at	---	13.7	202708_s_at	HIST2H2BE	-17.4
215767_at	ZNF804A	13.6	243386_at	CASZ1	-17.4
228790_at	FAM110B	13.5	241418_at	LOC344887	-17.2
1555793_a_at	ZFP82	13.5	223183_at	AGPAT3	-17.1
213808_at	---	13.5	228360_at	LYPD6B	-17.1
1557348_at	---	13.4	205206_at	KAL1	-17.1
220034_at	IRAK3	13.3	229450_at	IFIT3	-17.1
229437_at	MIR155HG	13.3	229154_at	LOC100288883	-17.0
207012_at	MMP16	13.3	203009_at	BCAM	-16.9
1557129_a_at	FAM111B	13.2	1558378_a_at	AHNAK2	-16.9
218332_at	BEX1	13.1	205064_at	SPRR1B	-16.7
1560297_at	---	13.1	229276_at	IGSF9	-16.6
202664_at	WIPF1	13.0	234931_at	---	-16.4
209094_at	DDAH1	13.0	230526_at	LOC100131096	-16.4
205499_at	SRPX2	13.0	209348_s_at	MAF	-16.4
223785_at	FANCI	12.8	202350_s_at	MATN2	-16.3
241710_at	LOC728819	12.7	222793_at	DDX58	-16.2
204629_at	PARVB	12.6	227752_at	SPTLC3	-16.2
204298_s_at	LOX	12.6	230323_s_at	TMEM45B	-16.2
212336_at	EPB41L1	12.6	226068_at	SYK	-16.0
203069_at	SV2A	12.6	236156_at	LIPA	-16.0
222161_at	NAALAD2	12.5	218723_s_at	C13orf15	-15.9
211767_at	GINS4	12.4	208153_s_at	FAT2	-15.9
204401_at	KCNN4	12.3	240218_at	DSCAM	-15.8
201860_s_at	PLAT	12.3	1555724_s_at	TAGLN	-15.8
206115_at	EGR3	12.2	242281_at	GLUL	-15.8
210319_x_at	MSX2	12.2	208284_x_at	GGT1	-15.8
230006_s_at	SVIP	12.1	202454_s_at	ERBB3	-15.6
201710_at	MYBL2	12.1	223980_s_at	SP110	-15.6
221024_s_at	SLC2A10	11.9	225283_at	ARRDC4	-15.5
231078_at	---	11.9	202037_s_at	SFRP1	-15.3
214102_at	ARAP2	11.8	238617_at	---	-15.3
243907_at	---	11.8	225618_at	ARHGAP27	-15.3
1560425_s_at	---	11.6	205660_at	OASL	-15.1
229465_s_at	---	11.5	1405_i_at	CCL5	-14.9
205943_at	TDO2	11.4	226576_at	ARHGAP26	-14.8
235588_at	ESCO2	11.4	1564383_s_at	FLJ35934	-14.8
1559400_s_at	PAPPA	11.4	219764_at	FZD10	-14.8

Upregulated (> 10-fold)			Downregulated (> 10-fold)		
213068_at	DPT	11.3	1559883_s_at	SAMHD1	-14.7
205476_at	CCL20	11.3	230788_at	GCNT2	-14.7
1566967_at	---	11.2	211890_x_at	CAPN3	-14.5
214079_at	DHRS2	11.2	232729_at	---	-14.5
236358_at	---	11.2	225286_at	ARSD	-14.4
1557217_a_at	FANCB	11.1	222016_s_at	ZNF323	-14.3
201508_at	IGFBP4	11.1	227498_at	SOX6	-14.1
207554_x_at	TBXA2R	10.9	49452_at	ACACB	-14.0
219911_s_at	SLCO4A1	10.9	224172_at	---	-14.0
235318_at	FBN1	10.7	227061_at	---	-14.0
210807_s_at	SLC16A7	10.6	226757_at	IFIT2	-14.0
209392_at	ENPP2	10.6	204070_at	RARRES3	-13.9
225516_at	SLC7A2	10.5	213832_at	KCND3	-13.9
235494_at	LSAMP	10.5	211654_x_at	HLA-DQB1	-13.9
1559382_at	C19orf42	10.5	236052_at	TRNP1	-13.8
202888_s_at	ANPEP	10.5	206582_s_at	GPR56	-13.8
1569053_at	AP3M2	10.4	210445_at	FABP6	-13.7
219733_s_at	SLC27A5	10.4	1558212_at	FLJ35024	-13.7
201116_s_at	CPE	10.3	212657_s_at	IL1RN	-13.6
223707_at	RPL27A	10.3	211484_s_at	DSCAM	-13.5
209101_at	CTGF	10.3	218280_x_at	HIST2H2AA3[#5]	-13.4
226991_at	NFATC2	10.2	235352_at	---	-13.3
204836_at	GLDC	10.1	225987_at	STEAP4	-13.3
228551_at	DENND5B	10.1	1554897_s_at	RHBDL2	-13.3
236539_at	PTPN22	10.0	204750_s_at	DSC2	-13.2
242260_at	MATR3	10.0	1554980_a_at	ATF3	-13.2
			218400_at	OAS3	-13.2
			205483_s_at	ISG15	-13.2
			229996_s_at	PCGF5	-13.1
			226603_at	SAMD9L	-13.1
			209283_at	CRYAB	-13.1
			226122_at	PLEKHG1	-13.1
			220664_at	SPRR2C	-13.1
			216258_s_at	SERPINB13	-13.0
			219090_at	SLC24A3	-13.0
			203936_s_at	MMP9	-13.0
			205680_at	MMP10	-12.9
			204503_at	EVPL	-12.9
			241455_at	C6orf132	-12.8
			243515_at	---	-12.8

	Downregulated (> 10-fold)		
	205125_at	PLCD1	-12.8
	239085_at	JDP2	-12.7
	201141_at	GPNMB	-12.7
	1559606_at	GBP6	-12.7
	205286_at	TFAP2C	-12.6
	219756_s_at	POF1B	-12.6
	215808_at	KLK10	-12.6
	225241_at	CCDC80	-12.5
	210128_s_at	LTB4R	-12.5
	223220_s_at	PARP9	-12.5
	1555786_s_at	C14orf34	-12.5
	211417_x_at	GGT1	-12.5
	225990_at	BOC	-12.4
	209828_s_at	IL16	-12.4
	236201_at	---	-12.4
	219597_s_at	DUOX1	-12.4
	219995_s_at	ZNF750	-12.4
	229909_at	B4GALNT3	-12.3
	220723_s_at	CWH43	-12.3
	218279_s_at	HIST2H2AA3	-12.3
	220225_at	IRX4	-12.3
	231236_at	ZFP57	-12.3
	206371_at	FOLR3	-12.1
	239062_at	LOC100131096	-12.0
	209183_s_at	C10orf10	-12.0
	1552502_s_at	RHBDL2	-12.0
	205595_at	DSG3	-11.9
	236129_at	GALNT5	-11.9
	205778_at	KLK7	-11.9
	236489_at	GPR110	-11.8
	213361_at	TDRD7	-11.8
	223395_at	ABI3BP	-11.7
	233413_at	---	-11.7
	205019_s_at	VIPR1	-11.7
	230405_at	C5orf56	-11.7
	229125_at	KANK4	-11.7
	223385_at	CYP2S1	-11.7
	213661_at	PAMR1	-11.6
	222847_s_at	EGLN3	-11.6
	228439_at	BATF2	-11.5

	Downregulated (> 10-fold)		
	202504_at	TRIM29	-11.5
	209611_s_at	SLC1A4	-11.5
	213183_s_at	CDKN1C	-11.4
	209417_s_at	IFI35	-11.4
	240024_at	SEC14L2	-11.3
	1554648_a_at	DUOXA1	-11.3
	244379_at	C1orf224	-11.3
	211416_x_at	GGTLC1	-11.2
	223784_at	TMEM27	-11.2
	209640_at	PML	-11.1
	227497_at	SOX6	-11.1
	222383_s_at	ALOXE3	-11.0
	235842_at	---	-11.0
	213375_s_at	N4BP2L1	-10.9
	239273_s_at	MMP28	-10.9
	207540_s_at	SYK	-10.9
	227113_at	ADHFE1	-10.9
	224009_x_at	DHRS9	-10.9
	205403_at	IL1R2	-10.8
	239866_at	---	-10.7
	207291_at	PRRG4	-10.7
	243702_at	---	-10.7
	207048_at	SLC6A11	-10.7
	237986_at	---	-10.7
	214399_s_at	KRT4	-10.7
	233641_s_at	FAM167A	-10.7
	236480_at	---	-10.6
	209720_s_at	SERPINB3	-10.6
	205916_at	S100A7	-10.6
	232222_at	C18orf49	-10.6
	1555491_a_at	C19orf66	-10.5
	230430_at	ENTPD2	-10.5
	230822_at	TMEM61	-10.5
	205860_x_at	FOLH1	-10.4
	239061_at	TPRXL	-10.4
	227091_at	CCDC146	-10.4
	225746_at	RAB11FIP4	-10.4
	AFFX-HUMISGF3A/M97935_MB_at	STAT1	-10.4
	205450_at	PHKA1	-10.4

	Downregulated (> 10-fold)		
	237268_at	DSCAM	-10.3
	227449_at	EPHA4	-10.3
	238028_at	C6orf132	-10.3
	240265_at	TRAF3IP3	-10.3
	1555929_s_at	---	-10.3
	212925_at	C19orf21	-10.2
	227393_at	ANO9	-10.2
	1558846_at	PNLIPRP3	-10.2
	213820_s_at	STARD5	-10.2
	212504_at	DIP2C	-10.1
	229130_at	---	-10.1
	227488_at	MGC16121[#6]	-10.1
	210480_s_at	MYO6	-10.1
	240390_at	GALNT5	-10.0
	204288_s_at	SORBS2	-10.0
	57588_at	SLC24A3	-10.0

#1, /// UGT1A10 /// UGT1A3 /// UGT1A4 /// UGT1A5 /// UGT1A6 /// UGT1A7 /// UGT1A8 /// UGT1A9; #2, /// UGT1A10 /// UGT1A4 /// UGT1A6 /// UGT1A8 /// UGT1A9; #3, /// LGALS7B; #4, /// RBMY1B /// RBMY1D /// RBMY1E /// RBMY1F /// RBMY1J; #5, /// HIST2H2AA4; #6, /// MIR503.

ZEB1, *ZEB2*, *CDH2* and *ID1* were highlighted in green while *NOTCH3* and *KLF4* were highlighted in red as they were validated in **Fig. 6A** or described previously (1). Note that *CDH1* (E-cadherin) was not included as this table lists the genes showing > 10-fold changes only. *CDH1* (201130_s_at) was 8.9-fold downregulated upon NOTCH3 knockdown. There were 3901 genes showing > 2-fold changes ($P < 0.05$). The gene lists in this table were subjected to functional annotation clustering analysis using the DAVID Bioinformatics Resources 6.7, NIAID/NIH (9). The most clustered probe sets were highlighted in blue for upregulated genes (Enrichment Score: 3.58) and in yellow for downregulated gene (Enrichment score: 9.50). For example, *ZEB2*, *CDH2* (N-cadherin) and *ID1* belonged to a Gene Ontology “cell motion” along with genes such as *IL6*, *FGF2* and *PTGS2* (i.e. cyclooxygenase-2), all essential factors implicated in EMT (10). *KLF4* constituted a Gene Ontology identity “epidermal cell differentiation” along with other genes such as *IVL* (Involucrin).

Supplementary References

1. Ohashi S, Natsuizaka M, Yashiro-Ohtani Y, Kalman RA, Nakagawa M, Wu L, et al. NOTCH1 and NOTCH3 coordinate esophageal squamous differentiation through a CSL-dependent transcriptional network. Gastroenterology. 2010;139:2113-23.

2. Jeffries S, Capobianco AJ. Neoplastic transformation by Notch requires nuclear localization. Mol Cell Biol. 2000;20:3928-41.

3. Ong CT, Cheng HT, Chang LW, Ohtsuka T, Kageyama R, Stormo GD, et al. Target selectivity of vertebrate notch proteins. Collaboration between discrete domains and CSL-binding site architecture determines activation probability. J Biol Chem. 2006;281:5106-19.

4. Andl CD, Mizushima T, Nakagawa H, Oyama K, Harada H, Chruma K, et al. Epidermal growth factor receptor mediates increased cell proliferation, migration, and aggregation in esophageal keratinocytes in vitro and in vivo. J Biol Chem. 2003;278:1824-30.

5. Okawa T, Michaylira CZ, Kalabis J, Stairs DB, Nakagawa H, Andl CD, et al. The functional interplay between EGFR overexpression, hTERT activation, and p53 mutation in esophageal epithelial cells with activation of stromal fibroblasts induces tumor development, invasion, and differentiation. Genes Dev. 2007;21:2788-803.

6. Harada H, Nakagawa H, Oyama K, Takaoka M, Andl CD, Jacobmeier B, et al. Telomerase induces immortalization of human esophageal keratinocytes without p16INK4a inactivation. Mol Cancer Res. 2003;1:729-38.

7. Kim SH, Nakagawa H, Navaraj A, Naomoto Y, Klein-Szanto AJ, Rustgi AK, et al. Tumorigenic conversion of primary human esophageal epithelial cells using oncogene combinations in the absence of exogenous Ras. Cancer Res. 2006;66:10415-24.

8. Darling DS, Stearman RP, Qi Y, Qiu MS, Feller JP. Expression of Zfhep/deltaEF1 protein in palate, neural progenitors, and differentiated neurons. Gene Expr Patterns. 2003;3:709-17.

9. Huang da W, Sherman BT, Lempicki RA. Systematic and integrative analysis of large gene lists using DAVID bioinformatics resources. Nat Protoc. 2009;4:44-57.

10. Thiery JP, Acloque H, Huang RY, Nieto MA. Epithelial-mesenchymal transitions in development and disease. Cell. 2009;139:871-90.